Donkey anti-Goat IgG (H+L) Cross-Adsorbed Secondary Antibody, Alexa Fluor™ 568

Product Details	
Size	1 mg
Species Reactivity	Goat
Host/Isotype	Donkey / IgG
Class	Polyclonal
Type	Secondary Antibody
Conjugate	Alexa Fluor™ 568
Excitation/Emission Max	579/603 nm
Immunogen	Gamma Immunoglobins Heavy and Light chains
Form	Liquid
Concentration	2 mg/mL
Purification	purified
Storage buffer	PBS, pH 7.5
Contains	5mM sodium azide
Storage conditions	4° C, store in dark
RRID	AB_2534104

Applications	Tested Dilution	Publications
Immunohistochemistry (IHC)	1-10 µg/mL	0 Publication
Immunohistochemistry (Paraffin) (IHC (P))	-	0 Publication
Immunohistochemistry (Frozen) (IHC (F))	-	0 Publication
Immunocytochemistry (ICC/IF)	1-10 µg/mL	0 Publication
Flow Cytometry (Flow)	1-10 µg/mL	0 Publication
Miscellaneous PubMed (Misc)	-	0 Publication

Product Specific Information

To minimize cross-reactivity, these donkey anti-goat IgG (H+L) whole secondary antibodies have been affinity purified and cross-adsorbed against rabbit, rat, mouse, and human IgG. Cross-adsorption or pre-adsorption is a purification step to increase specificity of the antibody resulting in higher sensitivity and less background staining. The secondary antibody solution is passed through a column matrix containing immobilized serum proteins from potentially cross-reactive species. Only the nonspecific-binding secondary antibodies are captured in the column, and the highly specific secondaries flow through. The benefits of this extra step are apparent in multiplexing/multicolor-staining experiments (e.g., flow cytometry) where there is potential cross-reactivity with other primary antibodies or in tissue/cell fluorescent staining experiments where there are may be the presence of endogenous immunoglobulins.

Alexa Fluor dyes are among the most trusted fluorescent dyes available today. Invitrogen™ Alexa Fluor 568 dye is a bright, orange/red-fluorescent dye with excitation ideally suited to the 568 nm laser line. For stable signal generation in imaging and flow cytometry, Alexa Fluor 568 dye is pH-insensitive over a wide molar range. Probes with high fluorescence quantum yield and high photostability allow detection of low-abundance biological structures with great sensitivity. Alexa Fluor 568 dye molecules can be attached to proteins at high molar ratios without significant self-quenching, enabling brighter conjugates and more sensitive detection. The degree of labeling for each conjugate is typically 2-8 fluorophore molecules per IgG molecule;

the exact degree of labeling is indicated on the certificate of analysis for each product lot.

Using conjugate solutions: Centrifuge the protein conjugate solution briefly in a microcentrifuge before use; add only the supernatant to the experiment. This step will help eliminate any protein aggregates that may have formed during storage, thereby reducing nonspecific background staining. Because staining protocols vary with application, the appropriate dilution of antibody should be determined empirically. For the fluorophore-labeled antibodies a final concentration of 1-10 µg/mL should be satisfactory for most immunohistochemistry and flow cytometry applications.

Product will be shipped at Room Temperature.

Product Images For Donkey anti-Goat IgG (H+L) Cross-Adsorbed Secondary Antibody, Alexa Fluor™ 568

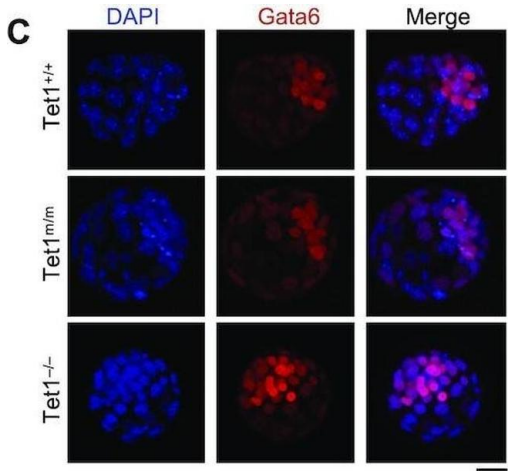

Goat IgG (H+L) Cross-Adsorbed Secondary Antibody (A-11057) in ICC/IF
Comparative analysis of Tet1+/+, Tet1m/m and Tet1/ blastocysts and mid-gestation embryos. (A) Unbiased quantification of blastocyst cell numbers by Volocity 3D Image Analysis software. n = 4 blastocysts per genotype were analyzed. Statistically significant * P < 0.05 (B) Quantification of Gata6 mRNA levels in blastocysts by RT-qPCR. n = 4 blastocysts of each genotype were analyzed. Data normalized to Gapdh. Error bars represent SEM. One way ANOVA test was used to assess statistically significant differences * P < 0.05. (C) Immunostaining for Gata6 (red) and nuclei (blue) in Tet1+/+, Tet1m/m and Tet1/ blastocysts. Scale bar = 27 µm. (D) Gross images of E9.5 embryos of the indicated Tet1 genotypes. Scale bar = 0.5 mm (E) Somite counts of E9.5 embryos of the indicated genotypes. Each dot represents an embryo. Error bars represent SD. One way ANOVA test was used to assess statistically significant differences * P < 0.05, ** P < 0.01. (F) Gross images of E11.5 embryos of the indicated Tet1 genotypes. Scale bar = 1 mm (G) Weight of E11.5 embryos of the indicated genotypes. Each dot represents an embryo. Error bars represent SD. One way ANOVA test was used to assess statistically significant differences, ** P < 0.01, *** P < 0.001 (H) Schematic of breeding strategy for inducible deletion of Tet1 during embryogenesis. (I) PCR genotyping of em Image collected and cropped by CiteAb from the following publication (https://pubmed.ncbi.nlm.nih.gov/35150568), licensed under a CC BY license.

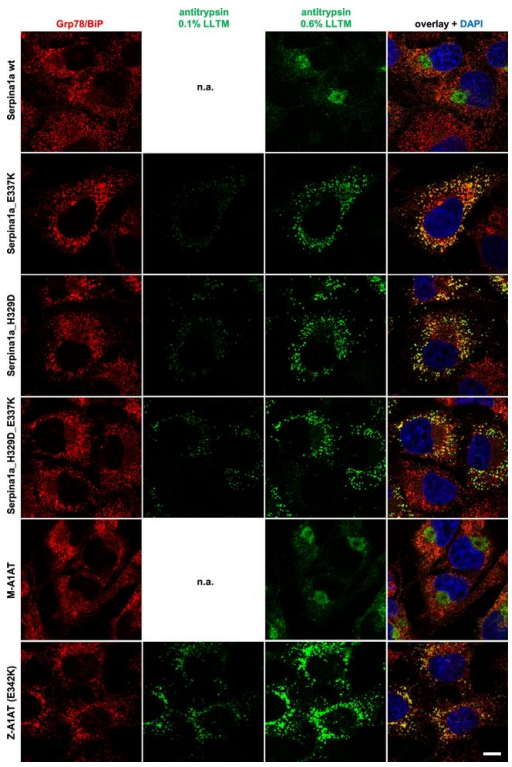

Goat IgG (H+L) Cross-Adsorbed Secondary Antibody (A-11057) in ICC/IF
Serpina1a mutants imitate intracellular distribution of human Z-A1AT. Confocal laser immunofluorescence analysis of COS-7 cells expressing wild type (wt; top row), E337K, H329D or H329D_E337K double mutant Serpina1a (second to fourth row), compared to cells overexpressing normal human M-A1AT or E342K Z-A1AT (fifth and sixth row). Mouse Serpina1a and human A1AT were stained with Alexa Fluor 568 secondary antibody (green) and exposed to 0.6% laser light transmission (LLTM). Mutant-expressing cells were additionally exposed to 0.1% LLTM, as the very strong signal resulted in over-saturation at 0.6%. ER-marker Grp78/BiP was stained with Alexa Fluor 647 secondary antibody (red) and cell nucleus was stained using DAPI (blue). Scale bar: 10 µm. Image collected and cropped by CiteAb from the following publication (http://www.nature.com/articles/s41598-019-44043-3), licensed under a CC BY license.

Goat IgG (H+L) Cross-Adsorbed Secondary Antibody (A-11057) in ICC/IF

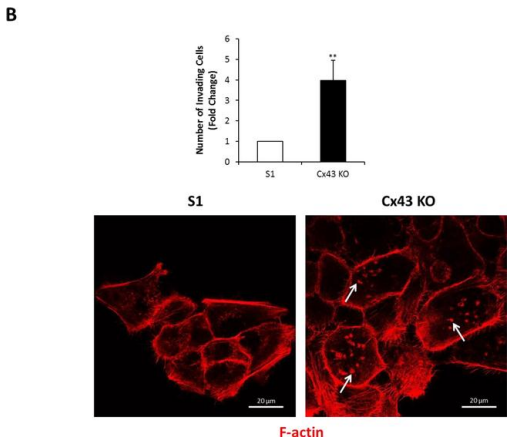

Silencing Cx43 induces motility and invasion in S1 cells. (A) S1 and Cx43-shRNA S1 cells (Cx43 KO) were cultured under 2-D conditions. Motility was assessed by time-lapse imaging on day 5. The total paths of representative S1 and Cx43 KO cells from time-lapse movies (upper panel) are shown (different colors represent different cells). Histograms show the quantification of cell motility. A total of 50 cells were analyzed per group. The values depicted are the means (±S.D.) of total path lengths (left lower panel) or migration speeds (right lower panel) from two independent experiments. Unpaired t-test; ** $p < 0.01$. (B) Invasion of S1 and Cx43 KO cells across diluted Matrigel (1:5) was assessed by transwell cell invasion assay (upper panel). The values depicted in the histogram are the means (±S.D.) of fold change in number of Matrigel-invading cells from three independent experiments. Unpaired t-test; ** $p < 0.01$. Representative images of cells cultured under 2-D conditions and stained for F-actin on day 5 (lower panel) are shown. Arrows indicate invadopodia-like actin-rich dots. (C) S1 and Cx43 KO cells were cultured under 3-D conditions atop of different Matrigel dilutions (undiluted, 1:5, 1:10 and 1:20 dilutions). Invasion was assessed by counting nonspheroid structures on day 11. One hundred structures were analyzed per group. The values depicted in the histogram (upper panel) are the means (±S.D.) of nons… Image collected and cropped by CiteAb from the following publication (https://pubmed.ncbi.nlm.nih.gov/30857262), licensed under a CC BY license.

View more figures on thermofisher.cn

996 References

Deciphering cartilage neuro-immune interactions and innervation profile through 3D engineered osteoarthritic micropathophysiological system. Mater Today Bio (2025)

Intrinsic electrical activity drives small-cell lung cancer progression. Nature (2025)

Generation of aNr2f2-driveninducible Cre mouse to target interstitial cells in the reproductive system bioRxiv (2025)

Real-time diagnostics and personalized wound therapy powered by AI and bioelectronics medRxiv (2025)

Presence of Gut Microbiota Worsens D-Galactosamine and Lipopolysaccharide-Induced Hepatic Injury in Mice. Genes Cells (2025)